ESMO GOOD SCIENCE BETTER MEDICINE BEST PRACTICE

ANNALS OF ONCOLOGY driving innovation in oncology

ORIGINAL ARTICLE

Fusobacterium nucleatum persistence and risk of recurrence after preoperative treatment in locally advanced rectal cancer

G. Serna[1], F. Ruiz-Pace[2], J. Hernando[3], L. Alonso[1], R. Fasani[1], S. Landolfi[4], R. Comas[2], J. Jimenez[1], E. Elez[3], S. Bullman[5], J. Tabernero[6], J. Capdevila[3], R. Dienstmann[2] & P. Nuciforo[1*]

[1]Molecular Oncology Group; [2]Oncology Data Science Group, Vall d'Hebron Institute of Oncology (VHIO), Barcelona; [3]Medical Oncology Department, Gastrointestinal and Endocrine Tumor Unit, Vall d'Hebron University Hospital, Vall Hebron Institute of Oncology (VHIO), Barcelona; [4]Department of Pathology, Vall d'Hebron University Hospital, Barcelona, Spain; [5]Human Biology Division, Fred Hutchinson Cancer Research Center, Seattle, USA; [6]Medical Oncology Department, Vall d'Hebron University Hospital, Vall d'Hebron Institute of Oncology (VHIO), IOB-Quiron, UVic-UCC, Barcelona, Spain

Available online 20 June 2020

Background: Accumulating evidence has identified *Fusobacterium* as an important pathogenic gut bacterium associated with colorectal cancer. Nevertheless, only limited data exist about the role of this bacterium in locally advanced rectal cancer (LARC). In this study, we quantified *Fusobacterium nucleatum* in untreated and post-neoadjuvant chemoradiotherapy (nCRT) samples from LARC patients and investigated its association with therapy response and survival.

Patients and methods: A total of 254 samples from 143 patients with rectal adenocarcinomas were analyzed for the presence and abundance of *F. nucleatum* using RNA *in situ* hybridization and digital image analysis. Assay accuracy was determined using infected cell lines and tumor samples with available quantitative PCR data. We studied the impact of *F. nucleatum* load on pathologic complete response and relapse-free survival. Treatment-induced changes were evaluated in paired pre- and post-nCRT samples ($n = 71$). Finally, tumor microenvironment changes during nCRT were assessed in paired samples ($n = 45$) by immune contexture analysis.

Results: *F. nucleatum* tissue levels by RNA *in situ* hybridization strongly correlated with quantitative PCR ($r = 0.804$, $P < 0.001$). *F. nucleatum* abundance was higher in untreated [median, 7.4; 95% confidence interval (3.7−16.2)] compared with treated [median, 1.6; 95% confidence interval (1.3−2.4)] tumors ($P < 0.001$) with 58% (73/126) and 26% (22/85) positive tumors, respectively ($P < 0.001$). Baseline *F. nucleatum* levels were not associated with pathologic complete response. *F. nucleatum* positivity after nCRT, but not baseline status, significantly increased risk of relapse [hazard ratio = 7.5, 95% confidence interval (3.0−19.0); $P < 0.001$]. Tumors that turned *F. nucleatum*-negative after nCRT had a strong increase in CD8+ T cells post-nCRT ($P < 0.001$), while those that persisted *F. nucleatum*-positive after nCRT lacked CD8+ T cells induction in post-nCRT samples compared with baseline ($P = 0.69$).

Conclusion: *F. nucleatum* persistence post-nCRT is associated with high relapse rates in LARC, potentially linked to suppression of immune cytotoxicity.

Key words: *Fusobacterium nucleatum*, locally advanced rectal cancer, microbiome, preoperative chemoradiotherapy

INTRODUCTION

Neoadjuvant chemoradiotherapy (nCRT) followed by total mesorectal surgical excision represent the standard treatment in patients with locally advanced rectal cancer (LARC). Patients receiving radiation therapy and fluoropyrimidine-based concurrent nCRT show improved rates of tumor downstaging and local control.[1] Multiple studies have shown reduced local relapse rates and improved patient survival rates after nCRT as compared with adjuvant treatment alone,[1,2] particularly when radiographic and/or pathologic complete response (pCR) is achieved.[3–6] However, only one-third of patients achieve pCR with nCRT, and those with either minimal regression or complete lack of response have a substantial risk of recurrence.[3,7]

The mechanisms underlying the observed heterogeneity of tumor sensitivity to nCRT are not well understood, and biomarkers to predict response to nCRT or relapse after optimal treatment of those not achieving pCR remain an unmet clinical need. A range of clinical, radiologic, serologic, histopathologic, immunologic, and genetic factors have been studied as potential predictors of response to nCRT in

*Correspondence to: Dr Paolo Nuciforo, Molecular Oncology Group, Vall d'Hebron Institute of Oncology (VHIO), CENTRE CELLEX, C/ Natzaret, 115-117, 08035 Barcelona, Spain. Tel: +34-93-254-34-50 Ext 8626
E-mail: pnuciforo@vhio.net (P. Nuciforo).

LARC.[8–12] More recently, the gut microbiota is increasingly recognized as having an important role in human colorectal cancer (CRC) development and progression[13–15] playing an intricate role in the modulation of the efficacy of a number of therapeutic approaches against cancer.[16,17]

Fusobacterium nucleatum is an important pathogenic gut bacterium associated with CRC.[18,19] The presence of *F. nucleatum* positively correlates with proximal tumor location, microsatellite instable tumors and higher CRC-specific mortality.[20] We have recently shown that treatment of *Fusobacterium*-harboring patient-derived xenografts with the antibiotic metronidazole decreases *Fusobacterium* load, cancer cell proliferation, and tumor growth.[21] In addition, *Fusobacterium* may promote CRC chemoresistance to oxaliplatin and fluorouracil (5-FU) regimens by modulating autophagy[22] in line with clinical data showing an association between a high amount of *F. nucleatum* and poor outcomes.[20] However, information on *F. nucleatum* abundance in LARC and the impact of CRT on the bacterium tissue levels is limited. Whether *F. nucleatum* positivity at baseline affects response to nCRT, or its persistence in residual tumor at surgery associates with relapse is unknown.

In this study, we evaluated the prevalence, patterns, and clinicopathological characteristics of *F. nucleatum* infection in LARC by high resolution *in situ* analyses conducted in primary tumor samples collected before and after nCRT and compared with those observed in a control cohort of untreated patients. We also assessed the ability of intratumoral *F. nucleatum* status determined in pre- and post-treatment tissue samples to predict the response in patients with LARC treated with nCRT and long-term prognosis. Finally, we looked at the relationship between *F. nucleatum* and immune cells in the tumor microenvironment.

METHODS

Patients and samples

The study group comprised 143 non-consecutive patients who were diagnosed with rectal adenocarcinomas at Vall d'Hebron University Hospital between 2007 and 2018 and who had available tissue for analysis. Eighty-seven patients had LARC treated with nCRT. LARC was defined as by T3/4 and/or node-positive tumors within 15 cm of the anal verge on rigid sigmoidoscopy and tumors below or at anterior peritoneal reflection defined by magnetic resonance imaging (MRI), without evidence of distance metastasis. Treatment response to nCRT was classified based on the tumor regression system. pCR was defined as the absence of any residual invasive tumor in the surgical resection specimen (GR0). GR0 and GR1 (near complete) response were classified as nCRT responders; GR2 as intermediate responders; and GR3 to GR5 as no responders. The control cohort included 56 patients with stages I to III rectal cancer who did not receive preoperative treatment given the tumor stage at diagnosis (stage I, low risk stage II upper rectal cancer), emergency surgery, or ineligibility for radiotherapy treatment (i.e. previous pelvic radiotherapy for prostate or cervix neoplasms). All patients undergoing surgery were administered metronidazole prophylaxis between 0 and 2 h before the procedure. The study was approved by the Vall d'Hebron University Hospital institutional ethical review board.

F. nucleatum in situ hybridization and image analysis

RNA *in situ* hybridization (RNA-ISH) was conducted using the RNAscope® technology (see supplementary Material, available at *Annals of Oncology* online). RNA-ISH stained slides were digitalized for signal quantification using a custom-made algorithm that automatically detected and counted individual and clustered red signals corresponding to bacteria mRNA molecules within a determined tumor region of interest. Whenever possible, a region of interest corresponding to adjacent normal rectal mucosa was drawn and included in the analysis. Results were expressed in density values (number of bacterial cells per mm^2 of tissue). Assay specificity was determined using HCT116 cell lines infected with increasing dose of *F. nucleatum* (multiplicity of infection: 0, 1, 10, 100) previously used in Bullman et al.[21] For comparative analysis between RNA-ISH and quantitative PCR (qPCR), we used qPCR data from 71 CRC samples of the 'formalin-fixed, paraffin-embedded (FFPE) paired cohort' studied in Bullman et al.[21] (see supplementary Material, available at *Annals of Oncology* online).

Immunohistochemistry

Immunohistochemistry (IHC) was carried out on consecutive sections using CD3, CD8, programmed death-ligand 1 (PD-L1) and pan-keratin antibodies (supplementary Table S1, available at *Annals of Oncology* online). The entire process was carried out in the Benchmark ULTRA system and all reagents were from Ventana Medical Systems, Tucson, AZ (see supplementary Material, available at *Annals of Oncology* online). Slides were digitalized using a slide scanner and quality checked by a pathologist before digital image analysis (DIA). For immunohistochemistry staining quantification, we used different DIA algorithms (see supplementary Material, available at *Annals of Oncology* online). In the case of CD3 and CD8, densities of intratumoral and peritumoral stained immune cells were calculated. For PD-L1 analysis, the combined positive score (CPS) was calculated by dividing the number of PD-L1-positive cells by the total number of pan-keratin-positive tumor cells multiplied by 100.

Statistical analyses

Continuous variables were expressed as median and interquartile range (IQR) or range (min-max). Categorical variables were expressed as absolute values and percentages. The median was used as a cut-off point for categorical variables (immune cells density). For *F. nucleatum*, the arbitrary cut-off of four bacteria cells/mm^2 of tissue was used to define *F. nucleatum*-positive versus *F. nucleatum*-negative tumors. This *F. nucleatum* positivity cut-off was defined before any clinical outcome data were explored based on validation studies in cell lines and tissues.

Comparison of continuous variables was carried out with the non-parametric Mann–Whitney *U* test (two groups), Wilcoxon rank sum test (two groups of paired samples) or Kruskal–Wallis test (more than two groups) with adjustment for multiple testing according to the Bonferroni method. Spearman correlation analysis was used to compare two continuous variables. For the univariate analysis of categorical variables, we used the chi-square test or Fisher's exact test and the McNemar test for paired samples. Responders were defined as patients achieving complete response (GR0) or near complete response (GR1) after nCRT. Relapse-free survival (RFS) was calculated from the date of surgery of primary tumor to first relapse (either local or distant) or last follow up date (censoring). Survival analysis was calculated using the Kaplan–Meier method and log-rank test was used for statistical comparison. Cox proportional-hazard models were used to obtain hazard ratios (HRs) with 95% confidence intervals (CI). Statistical significance was accepted at the conventional two-sided $P < 0.05$ thresholds. All analyses were carried out using R version 3.6.2 statistical software package, Vienna, Austria.

RESULTS

Optimized RNA-ISH assay for intratumoral *F. nucleatum* detection within intact tissue

To develop an automated RNA-ISH workflow enabling simultaneous visualization and quantification of bacteria within the tissue context in FFPE sections, we built upon a methodology originally developed in our laboratory for *F. nucleatum* visualization[21] and subsequently automatized both the technical and analytical steps to enable robust determination of intratumoral bacteria content. Briefly, the assay used chromogenic RNA-ISH combined with DIA to allow for automatic counting of bacteria. In order to verify that the RNA-ISH assay could specifically detect *F. nucleatum* at the expected density, we used HCT116 cell lines infected with increasing dose of *F. nucleatum* (multiplicity of infection: 0, 1, 10, 100). Mean (range) *F. nucleatum* densities were 2.4 (1.5–3.8), 1246.7 (1054.5–1598.8), 4552.6 (4055.3–5016), and 36728.8 (25744–47147.6) in cell lines infected with 0, 1, 10, and 100, respectively (Figure 1A and B, supplementary Table S2, available at *Annals of Oncology* online). We then investigated whether the method could provide reliable quantitative expression data on FFPE human CRC samples by performing a parallel analysis of the bacteria tissue abundance by qPCR and RNA-ISH. Data obtained with the two methods were highly concordant (ISH versus qPCR, Pearson correlation 0.804, $P < 0.001$, Figure 1C). The agreement rate of the two methods in classifying a tumor according to *F. nucleatum* status was 86% (Fisher's exact test, $P < 0.001$, supplementary Table S3, available at *Annals of Oncology* online).

Spatial analysis showed that *F. nucleatum* was mainly localized at the luminal surface of the tumor. Bacteria usually aggregated together forming cluster signals which were found freely distributed within the intestinal lumen (Figure 1D), adherent to necrotic tissue in ulcerated tumors (Figure 1E) or directly to tumor cells with individual bacteria invasion (Figure 1F).

Patient characteristics

The study included 143 patients (Table 1, supplementary Figure S1, available at *Annals of Oncology* online). Males represented 61.5% of the population. The median age at diagnosis was 71 years (range, 45–90). All tumors were diagnosed as adenocarcinomas. Eighty-seven patients received nCRT (treated cohort), which consisted of a combination of fluoropyrimidine (capecitabine 850 mg/m^2 twice daily, 7 days per week, from the first to the last day of radiotherapy) ($n = 69$, 79.3%) or short course radiotherapy alone using the schedule of 5 Gy for 5 consecutive days ($n = 18$, 20.7%). The median time from the end of nCRT to surgery was 9.9 weeks (range, 1.4–21.6). Eight patients (9.5%) had pCR (GR0), 13 patients (15.3%) had occasional microscopic foci of residual tumor (GR1), and 64 patients (75.3%) had intermediate or no tumor regression. In two patients (2.3%), regression grade was not available (supplementary Table S4, available at *Annals of Oncology* online). No significant associations between clinicopathological features and pathological response after nCRT or RFS were observed (supplementary Table S5, available at *Annals of Oncology* online). Fifty-six patients were included in the untreated control cohort. No significant differences in the patients' clinicopathological features were found between treated and untreated cohorts, with the exception of disease stage at diagnosis, as anticipated (Table 1).

F. nucleatum abundance in LARC

F. nucleatum was successfully evaluated in 251 out of 254 tumor samples (untreated, $n = 166/167$; treated, $n = 85/87$). The median *F. nucleatum* density was 7.4 (IQR 2.1–52.0) in untreated samples and 1.6 (IQR 0.8–4.4) in post-nCRT samples (Mann–Whitney $P < 0.001$). When considering *F. nucleatum* as a categorical variable (positive versus negative), rates of *F. nucleatum* positivity were 57% and 25% in untreated and nCRT-treated tumors, respectively (Fisher's exact test $P < 0.001$).

Normal adjacent mucosa was evaluable for analysis in 36 samples (untreated, $n = 19$; treated, $n = 16$). Median *F. nucleatum* density in adjacent normal tissue was 0.3 (IQR, 0.0–0.9) with 0% of samples being positive (untreated tumors versus normal, $P < 0.001$; treated tumors versus normal, $P < 0.001$). *F. nucleatum* did not differ according to normal sample origin (untreated, median = 0.2; treated, median = 0.3; $P = 0.85$).

We did not find significant differences in the median densities or proportion of positive cases across sample types and cohorts (supplementary Table S6, available at *Annals of Oncology* online). A trend towards a higher median value in endoscopic samples as compared with untreated surgical specimens was observed ($P = 0.13$).

Lastly, we searched for associations between a patient's clinicopathological features and *F. nucleatum* status in untreated samples. No significant differences in *F. nucleatum*

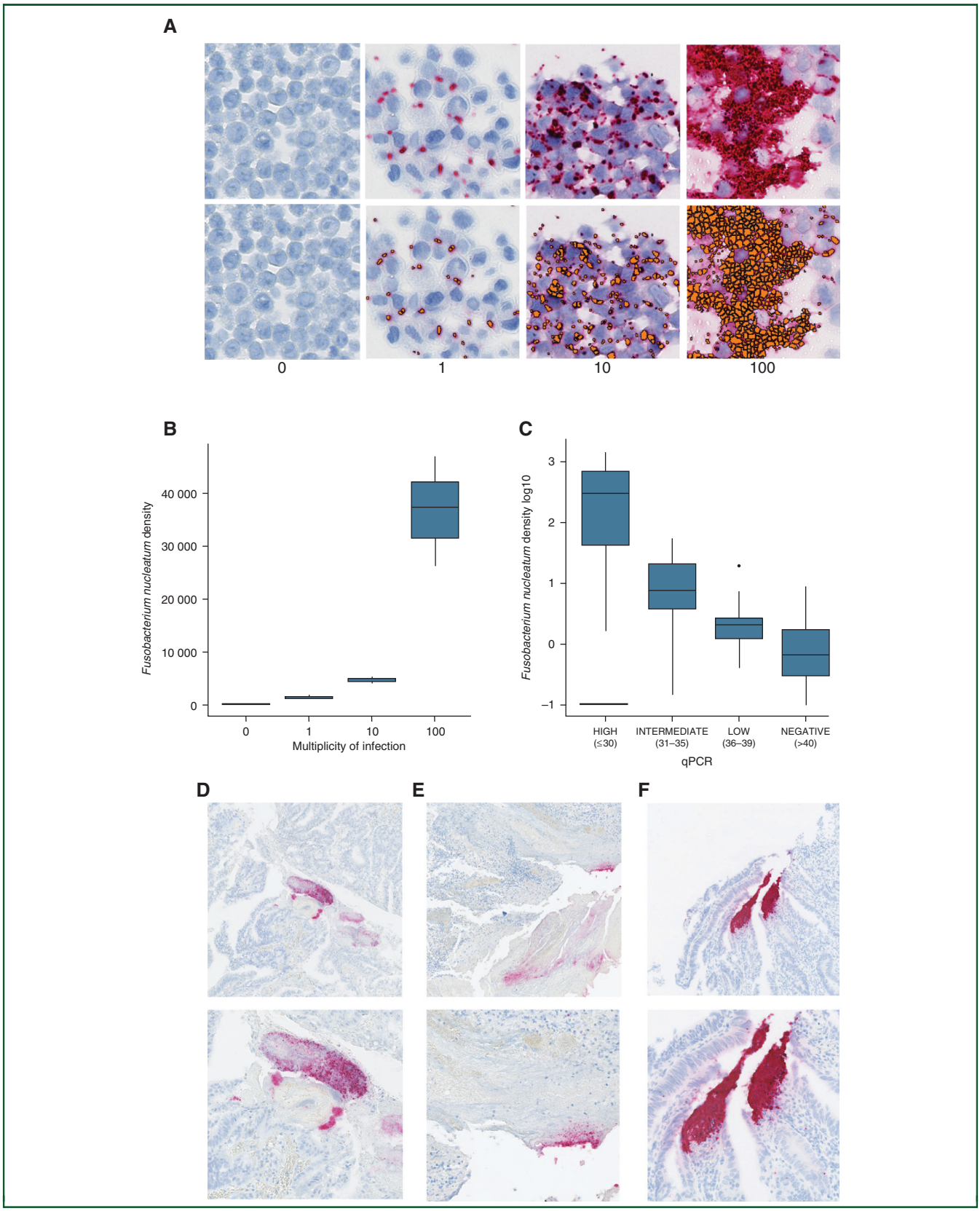

Figure 1. RNA-ISH assay for intratumoral *Fusobacterium nucleatum* visualization and quantification.
(A) Representative RNA-ISH images of HCT116 cell lines infected with increasing dose of *Fusobacterium nucleatum* (multiplicity of infection: 0, 1, 10, 100 from left to right; digital magnification, 30×). Upper: RNA-ISH; bottom: RNA-ISH after digital image analysis (DIA). (B) Boxplot of *F. nucleatum* densities quantification by DIA in infected cell lines (multiplicity of infection: 0, 1, 10, 100). (C) Boxplot of log10-transformed *Fusobacterium* densities by DIA by qPCR categories (high: ct value ≤30; intermediate: ct value 31—35; low: ct value 36—39 and negative: ct value >40). (D—F) Representative RNA-ISH images showing patterns of *F. nucleatum* infection in rectal cancer tissue samples (digital magnification, upper:10×, bottom: 30×). (D) Non-adhesive *F. nucleatum*; (E) adhesive *F. nucleatum* in correspondence of ulceration; (F) invasive *F. nucleatum*.
ISH, *in situ* hybridization; qPCR, quantitative PCR.

https://doi.org/10.1016/j.annonc.2020.06.003

Table 1. Clinicopathological variables description of included patients (left). Comparison of variables between treated and untreated patients (right).

Variables	All ($N = 143$)		Patients by neoadjuvant therapy		
			Treated ($N = 87$)	Untreated ($N = 56$)	Fisher's exact test
Age at diagnosis Median (range), years	71.4 (45.0–90.6)	**Age at diagnosis**	71.2 (48.7–86.7)	71.6 (45.0–90.6)	$P = 0.99$
Sex, *n* (%)		**Sex, *n* (%)**			$P = 0.86$
Male	88 (62)	Male	53 (60)	35 (40)	
Female	55 (38)	Female	34 (62)	21 (38)	
Histology, *n* (%)		**Histology, *n* (%)**			$P = 0.11$
Conventional	123 (88)	Conventional	78 (63)	45 (37)	
Mucinous	17 (12)	Mucinous	7 (41)	10 (59)	
Stage, *n* (%)		**Stage, *n* (%)**			$P < 0.001$
I	16 (11)	I	0 (0)	16 (100)	
II	23 (16)	II	7 (30)	16 (70)	
III	103 (73)	III	79 (77)	24 (23)	
Relapse, *n* (%)		**Relapse, *n* (%)**			$P = 0.39$
0	114 (80)	0	67 (59)	47 (41)	
1	29 (20)	1	20 (69)	9 (31)	
Survival, *n* (%)		**Survival, *n* (%)**			$P = 0.56$
Alive	105 (73)	Alive	62 (59)	43 (41)	
Dead	38 (27)	Dead	25 (66)	13 (34)	
		***Fusobacterium* (pre), *n* (%)**			$P = 0.15$
		Positive	45 (62)	28 (38)	
		Negative	25 (47)	28 (53)	
Time to surgery Median (95% CI) months	3.2 (2.4–4.4)	**Time to surgery** Median (95% CI) months	4.9 (4.6–5.1)	1.3 (1.1–1.6)	$P < 0.001$

CI, confidence interval.

positivity according to age, sex, stage, and histology were observed (supplementary Table S7, available at *Annals of Oncology* online).

Association of *F. nucleatum* with response to nCRT

We evaluated the association of pretreatment and post-treatment *F. nucleatum* with response after nCRT. *F. nucleatum* abundance at baseline was not predictive of pathological response, neither as a continuous nor as a categorical variable. Median *F. nucleatum* densities were 18.1 (0.6–4658) and 9.3 (0.0–1665) in responders and non-responders, respectively ($P = 0.27$). The rates of response in *F. nucleatum*-positive and *F. nucleatum*-negative tumors were 34% and 13%, respectively (odds ratio = 3.6, 95% CI 1.0–17.51, $P = 0.08$, supplementary Table S8, available at *Annals of Oncology* online).

A total of 85 patients had post-treatment surgically resected tumors with *F. nucleatum* data. There was no association between *F. nucleatum* status at surgery and response to nCRT. *F. nucleatum* remained positive in 10% of patients achieving response (GR0 and GR1) compared with 27% of those who did not responded ($P = 0.13$, supplementary Table S8, available at *Annals of Oncology* online).

Association of *F. nucleatum* with relapse after nCRT

In the control cohort, relapse rates were 21% and 11% in the *F. nucleatum*-positive and *F. nucleatum*-negative subgroups, respectively (HR = 2.2, 95% CI: 0.5–8.9, $P = 0.20$) (Figure 2A, supplementary Figure S2A, available at *Annals of Oncology* online). When considering stages II and III only in the control cohort, a trend towards worse outcomes was observed (HR = 5.8, 95% CI: 0.7–50.4, $P = 0.07$] (supplementary Figure S2B, available at *Annals of Oncology* online).

In the treated cohort, pretreatment *F. nucleatum* status was not a determinant of RFS after nCRT (HR = 0.9, 95% CI: 0.3–2.9, $P = 0.98$) (Figure 2B). On the other hand, when bacterium status was determined in post-treatment samples, the proportion of patients experiencing a relapse after nCRT was 59% (13/22) in the *F. nucleatum*-positive group and 11% (7/63) in the negative subgroups, respectively (odds ratio = 11.6, 95% CI: 3.2–43.3, $P < 0.001$) determined in post-treatment samples. The median RFS was 21 months (12.5–not reached) and not reached in the *F. nucleatum*-positive and *F. nucleatum*-negative subgroups, respectively (HR = 7.5, 95% CI: 3.0–19.0, $P < 0.001$) (Figure 2C). In a survival model adjusting for preoperative treatment regimen (CRT versus radiotherapy only), the association between post-treatment *F. nucleatum* status and prognosis was maintained (supplementary Table S9, available at *Annals of Oncology* online).

As pCR is a known prognostic marker after nCRT, we carried out the same survival analysis after excluding patients who experienced pCR. Post-nCRT *F. nucleatum* status remained a significant predictive marker for RFS with *F. nucleatum*-positive patients showing a significantly higher risk of developing a later recurrence after nCRT (HR = 7.1, 95% CI: 2.8–18.0, $P < 0.001$) (supplementary Figure S2C, available at *Annals of Oncology* online).

Treatment-associated changes of *F. nucleatum* in paired samples

A total of 71 patients had paired pre- and post-nCRT samples with *F. nucleatum* data. Compared with untreated biopsy samples, levels of *F. nucleatum* at surgery were

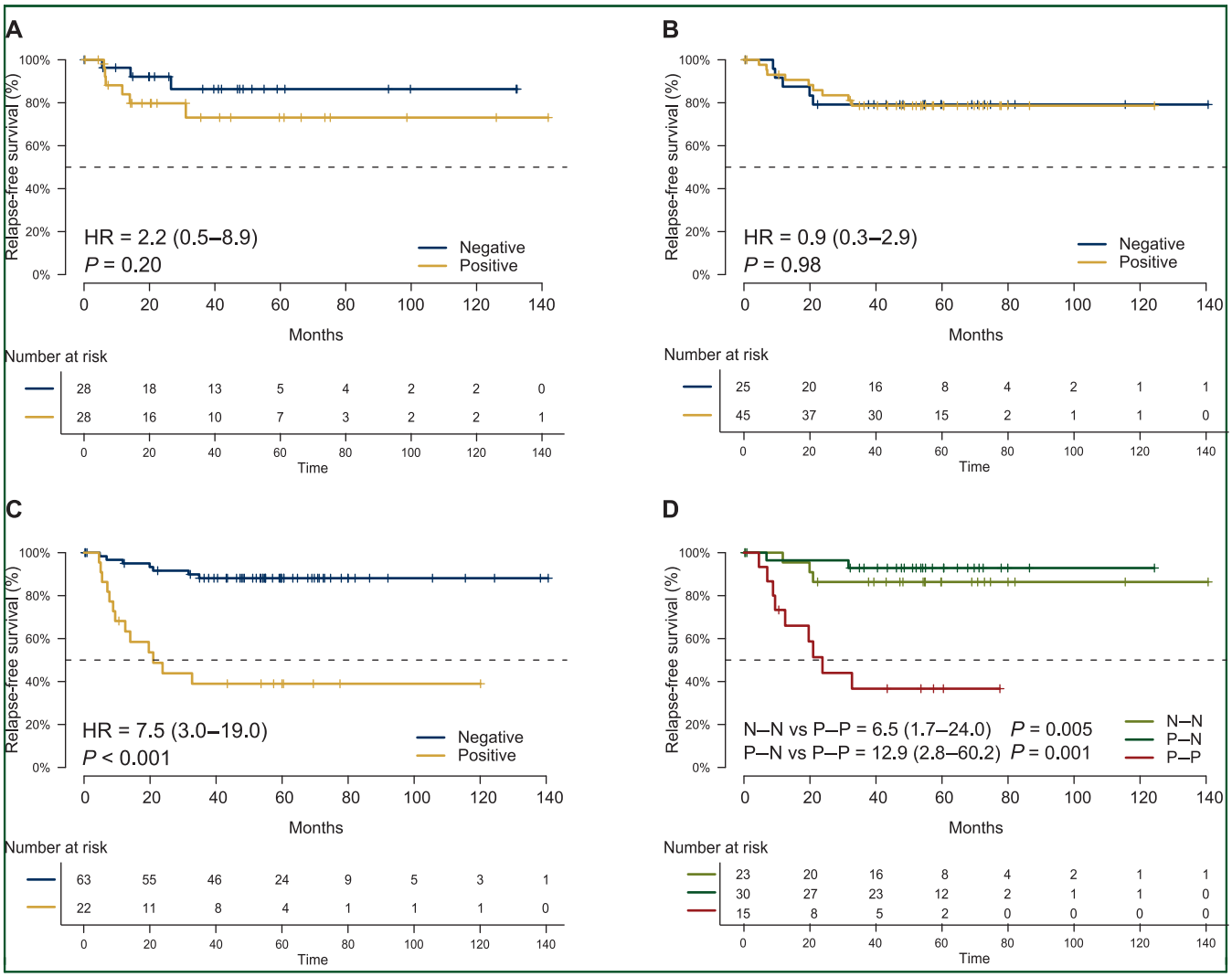

Figure 2. Kaplan–Meier curves for relapse-free survival (RFS).
(A) Control cohort by *Fusobacterium nucleatum* baseline status. (B) Treated cohort by *F. nucleatum* status in pre-neoadjuvant chemoradiotherapy (nCRT) tumor samples. (C) Treated cohort by *F. nucleatum* status in post-nCRT tumor samples. (D) Paired treated cohort grouped according to the shift in *F. nucleatum* status between pre-nCRT and post-nCRT paired samples. N-N: patients who maintained negative *F. nucleatum* status before and after treatment. P-N: patients in whom *F. nucleatum* was negative after treatment. P-P: patients with a positive *F. nucleatum* status in both samples.
HR, hazard ratio.

significantly lower (median, untreated = 13.5 and treated = 1.5, $P < 0.001$). The proportion of *F. nucleatum* positivity significantly dropped from 67.1% to 21.7% upon treatment (Fisher's exact test, $P < 0.001$).

All tumors that were negative at baseline were also negative after nCRT (N-N, $n = 23$, 34%). Among *F. nucleatum*-positive tumors at baseline, 44% changed *F. nucleatum* status from positive to negative (P-N, $n = 30$) while 22% remained positive in the post-nCRT sample (P-P, $n = 15$) (McNemar test, $P < 0.001$). Patients with P-P tumors had a higher risk of developing a relapse (HR = 9.0, 95% CI: 3.0–27.2, $P < 0.001$) as compared with tumors that were negative (N-N) or negativized (P-N) upon treatment (Figure 2D, supplementary Figure S3, and supplementary Table S10, available at *Annals of Oncology* online). The interval between the end of nCRT and surgery did not impact on *F. nucleatum* status group change (supplementary Figure S4, available at *Annals of Oncology* online).

F. nucleatum and immune microenvironment

Among 71 patients from the treated cohort with paired pre- and post-nCRT samples, 45 had immune cells content data. Median pretreatment densities of CD3+ and CD8+ cells were 1023.5 (IQR 745.8–1326.0) and 119.0 (IQR 70.0–167.0), respectively. Median PD-L1 CPS was 14.3 (IQR 6.0–20.5). Tumor-infiltrating lymphocytes did not significantly differ according to *F. nucleatum* status in pretreatment samples ($P = 0.81$). After treatment, no significant changes in CD3+ (median density = 669, IQR 329.5–1301.8) and PD-L1 expression (median CPS = 3.9, IQR 1.2–12.7) were observed as compared with baseline ($P = 0.12$ and 0.15, respectively). In contrast, CD8+ immune infiltration increased significantly upon treatment (median = 312.0, IQR 183.0–726.0; $P < 0.001$). When stratifying post-treatment samples by *F. nucleatum* status, significant lower densities of all immune cell subtypes and PD-L1 expression were observed in *F. nucleatum*-positive compared with *F. nucleatum*-negative

https://doi.org/10.1016/j.annonc.2020.06.003

tumors (CD3, $P = 0.004$; CD8, $P = 0.001$; PD-L1, $P = 0.02$) (Table 2, supplementary Figure S5, available at *Annals of Oncology* online).

Then, to better understand the interaction between *F. nucleatum* and immune microenvironment during nCRT, we investigated CD8+ immune cells densities in the three different patient subgroups that consider the changes in *F. nucleatum* status pre- and post-nCRT (N-N, P-N, and P-P). Median CD8+ cells densities did not differ significantly across groups in pretreatment samples (104, 119, and 82 in N-N, P-N, and P-P, respectively, $P = 0.69$). In post-treatment samples, median CD8+ density was significantly higher in N-N and P-N (440 and 532, respectively) as compared with P-P (163) tumors ($P = 0.006$). Intra-group comparison showed post-treatment CD8+ increase in N-N ($P = 0.01$) and P-N ($P < 0.001$) tumors but not in P-P tumors ($P = 0.51$) (Figure 3).

DISCUSSION

To our knowledge, this is the first study to evaluate *F. nucleatum* changes in primary rectal cancer exposed to nCRT. Our data provide an opportunity to understand treatment-associated changes of tumor microenvironment in relation to *F. nucleatum* status between pre- and post-nCRT specimens and how these may affect a patient's outcome.

Fusobacterium is increasingly recognized as having an important role in human CRC carcinogenesis. In two seminal studies in which the microbial composition of tissue samples from CRCs were compared with matched normal colon specimens using genomic analyses, *Fusobacterium* abundance was the most significantly different bacteria between the two groups with *F. nucleatum* infection being prevalent in human CRC.[18,19] Since then, several studies have aimed to both confirm and strengthen this association. Collectively, these data have shown that *F. nucleatum*-positive tumors may represent a distinct CRC subgroup correlated with proximal location, microsatellite instability, and worse prognosis.[23,24]

No previous studies have specifically addressed the prevalence, prognostic, and predictive roles of *F. nucleatum* in LARC. In the largest retrospective analysis of *F. nucleatum* conducted on 1102 CRCs using quantitative PCR, rectal cancers ($n = 157$) exhibited the lowest proportion of *F. nucleatum*-high tumors (2.5%).[25] However, the global prevalence (including tumor with both high and low bacterial DNA content by PCR) was 12.5%, which was not significantly different from tumors originating from proximal colon ($n = 536$, 15.6%, $P = 0.365$).

In our study, the positivity rate of intratumoral *F. nucleatum* infection in LARC was 57%, which is higher than the one reported in the USA cohort, but in line with prevalence data from other CRC studies.[26,27] Factors including geography, ethnicity, experimental methodology used, and study cohort can explain the variability in the reported infection rates.[23,28,29]

For the first time, here we used an automatized version of the RNA-ISH assay we originally developed for bacteria visualization in matched primary and metastatic CRC intact FFPE tissues.[21] Beyond providing reliable quantitative information on bacterial tissue content, this assay brings spatial information by unveiling how *F. nucleatum* interacts with host cells within the tumor microenvironment.

Personalization of treatments in LARC relies on the identification of prognostic and predictive biomarkers in patients undergoing nCRT, which remains an unmet clinical need.[30] Pretreatment *F. nucleatum* status did not impact on rectal cancer prognosis, although a trend for higher relapse was noticed in untreated stage II and III populations. We also observed that neither pretreatment nor post-treatment *F. nucleatum* was associated with response to nCRT, thus limiting its use as a predictive biomarker of pCR.

More importantly, the presence of bacteria in post-treatment samples was significantly associated with a higher risk of relapse. Our data show that chemotherapy and radiation are able to significantly reduce the intratumoral content of *F. nucleatum* and to induce a tumor to shift from an *F. nucleatum*-positive to an *F. nucleatum*-negative status in two-thirds of cases. Tumors changing their '*microbiotype*' from positive to negative behaved as *F. nucleatum*-negative tumors and showed improved RFS. On the other hand, those tumors that remained *F. nucleatum*-positive after preoperative CRT had a higher risk of developing a relapse during follow up. Interestingly, tumors that turned *F. nucleatum*-negative after nCRT had a strong increase in CD8+ T cells post-nCRT, while those that persisted *F. nucleatum*-positive after nCRT lacked CD8+

Table 2. Immune cells densities and programmed death-ligand 1 (PD-L1) expression data by sample type and *Fusobacterium nucleatum* status from paired treated cohort.

	Sample type	Median (IQR)	*P* value[a]	*Fusobacterium nucleatum* status		*P* value[b]
				Positive	Negative	
CD3+	Pre	1023.5 (745.8–1326.0)	0.12	1024.0 (760.0–1315.0)	1024.0 (583.5–1451.8)	0.95
	Post	669 (329.5–1301.8)		261.0 (175.8–387.0)	723.5 (147.0–1578.5)	0.004
CD8+	Pre	119.0 (70.0–167.0)	<0.001	119.0 (70.0–154.0)	114.5 (69.0–203.0)	0.81
	Post	312.0 (183.0–726.0)		163.0 (73.0–220.0)	486.0 (34.0–788.0)	0.001
PD-L1	Pre	14.3 (6.0–20.5)	0.15	14.3 (5.5–20.5)	13.9 (7.7–19.0)	0.97
	Post	3.9 (1.2–12.7)		1.1 (0.7–3.5)	5.9 (1.9–17.1)	0.02

[a] Wilcoxon test for paired samples.
[b] Mann–Whitney *U* test for unpaired samples.

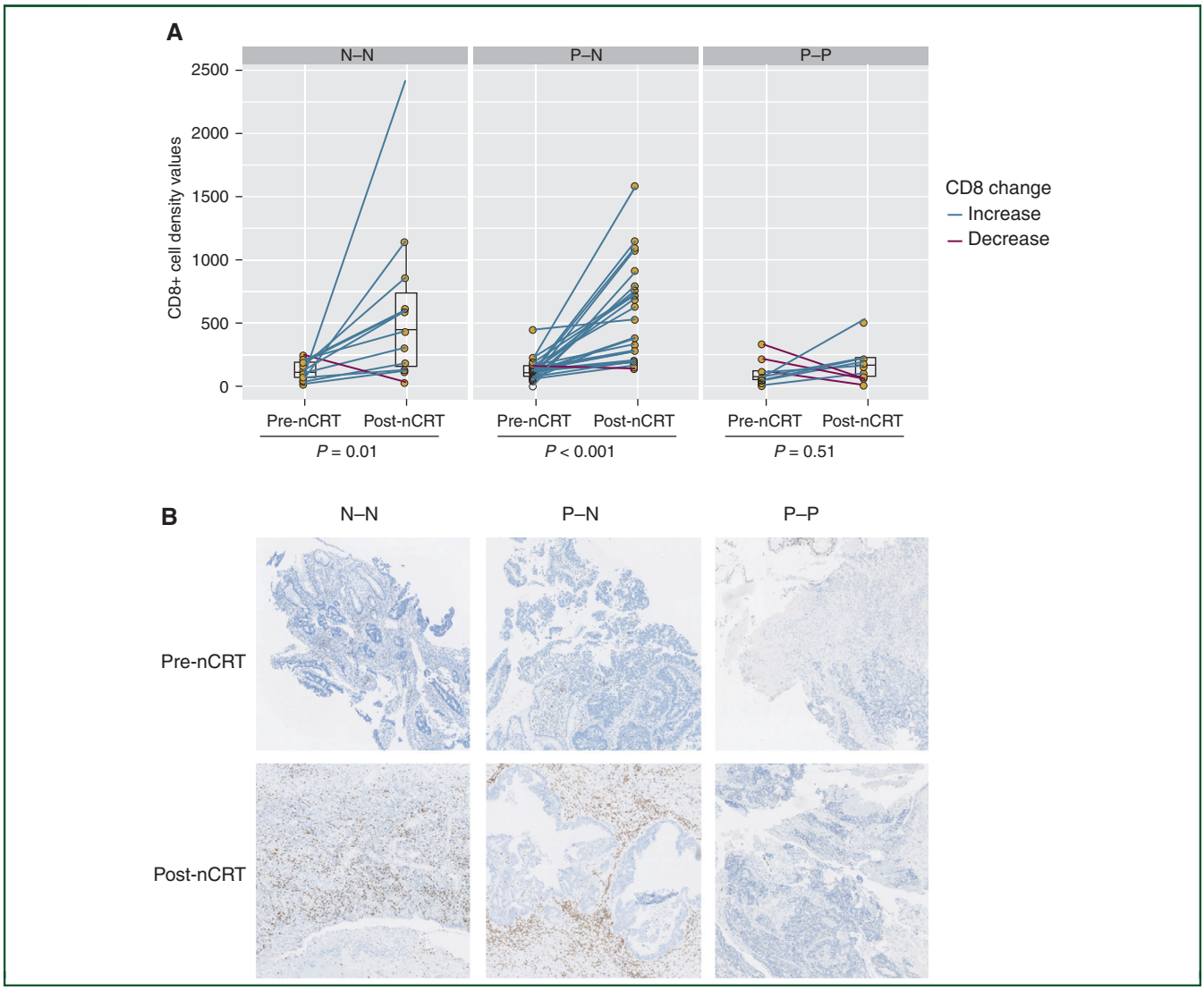

Figure 3. Tumor immune microenvironment modulation according to treatment-induced microbiotype status change.
(A) Multiple parallel coordinate plot and boxplot of the change of CD8+ cells density values in three groups of patients defined based on the change of *Fusobacterium nucleatum*status from pre-nCRT samples to post-nCRT samples (N-N, negative-negative; P-N, positive-negative; P-P positive-positive). Each line joins both samples belonging to the same patient. The blue lines highlight the increase in CD8+ while the pink lines indicate a decrease in these values. (B) Representative immunohistochemistry images of CD8 immune cells staining in pre-nCRT and post-nCRT paired samples (digital magnification, 10×).
nCRT, neoadjuvant chemoradiotherapy.

T cells induction in post-nCRT samples as compared with baseline.

Our observation of the differences in immune cell induction according to post-treatment *F. nucleatum* status suggests a possible mechanism of immunological mechanism for worse outcome linked to the bacterium. CRT may prime the immune system by a variety of underlying mechanisms including an increase in tumor mutation burden, creating appropriate mutations or neoantigens, which are not fully understood.[30,31] Other studies have shown that high tumor-infiltrating lymphocytes content in post-treatment surgical samples are associated with a better outcome in rectal cancer.[11,32] *F. nucleatum* is known to be immunosuppressive,[33–35] and that may play a role in chemoresistance and metastasization.[21,22] Our data suggest that this anti-inflammatory and pro-metastatic program may be particularly active in the context of nCRT, with *F. nucleatum* promoting immune escape leading to disease recurrence. One may hypothesize that patients with *F. nucleatum*-positive tumors may benefit from novel neoadjuvant or adjuvant treatment approaches that target this bacterium to reduce the risk of immune escape and metastatic seeding.

Our study has some weaknesses, including the small sample size composed of non-consecutive patients selected based on tissue and clinical data availability. Despite being retrospective, our study followed a prospectively defined protocol for data analysis based on the original research objective. Lastly, the association between *F. nucleatum* and immune microenvironment is hypothesis-generating in terms of mechanistic insights, but we cannot prove causation in this study. Hence, our results require validation in independent cohorts.

https://doi.org/10.1016/j.annonc.2020.06.003

In summary, our study creates a path forward by leveraging microbiome profiling for consideration of alternative nCRT strategies in patients with locally advanced rectal tumors. We provided useful information on the clinical applicability of *F. nucleatum* as prognostic tissue biomarker. We also suggested a possible mechanism through which *F. nucleatum* may promote immune suppression and favor metastatic spread in LARC, thus further connecting the microbiome of CRC to immune modulatory effects. Finally, our study highlights the great opportunity for additional investigations aimed to elucidate how targeting intratumoral *F. nucleatum* affects tumor growth and dissemination.

ACKNOWLEDGEMENTS

Acknowledgements to the Cellex Foundation for providing research facilities and equipment.

FUNDING

This work was supported by Cancer Research UK [grant number C17937/A29070] and by the Comprehensive Program of Cancer Immunotherapy & Immunology (CAIMI) BBVA Foundation [grant number 89/2017].

DISCLOSURE

JT reports personal financial interest in the form of scientific consultancy role for Array Biopharma, AstraZeneca, Bayer, BeiGene, Boehringer Ingelheim, Chugai, Genentech, Inc., Genmab A/S, Halozyme, Imugene Limited, Inflection Biosciences Limited, Ipsen, Kura Oncology, Lilly, Merck Sharp & Dohme, Menarini, Merck Serono, Merrimack, Merus, Molecular Partners, Novartis, Peptomyc, Pfizer, Pharmacyclics, ProteoDesign SL, Rafael Pharmaceuticals, F. Hoffmann-La Roche Ltd, Sanofi, SeaGen, Seattle Genetics, Servier, Symphogen, Taiho, VCN Biosciences, Biocartis, Foundation Medicine, HalioDX SAS, and Roche Diagnostics. JC reports scientific consultancy role (speaker and advisory roles) from Novartis, Pfizer, Ipsen, Exelixis, Bayer, Eisai, Advanced Accelerator Applications, Amgen, Sanofi, ITM, Sirlex and Merck Serono. Research grants from Novartis, Pfizer, AstraZeneca, Advanced Accelerator Applications, Eisai, and Bayer. RD has an advisory role at Roche and Boehringer-Ingelheim, has received a speaker's fee from Roche, Ipsen, Amgen, Sanofi, Servier, Merck Sharp & Dohme and further received direct research funding from Merck and Pierre Fabre. PN has consulted for Bayer, Novartis, Merck Sharp & Dohme, and Targos, and received compensation. The other authors have declared no conflicts of interest.

REFERENCES

1. Sauer R, Becker H, Hohenberger W, et al. Preoperative versus postoperative chemoradiotherapy for rectal cancer. *N Engl J Med*. 2004;351(17):1731—1740.
2. Bosset JF, Calais G, Mineur L, et al. Enhanced tumorocidal effect of chemotherapy with preoperative radiotherapy for rectal cancer: preliminary results - EORTC 22921. *J Clin Oncol*. 2005;23(24):5620—5627.
3. Park IJ, You YN, Agarwal A, et al. Neoadjuvant treatment response as an early response indicator for patients with rectal cancer. *J Clin Oncol*. 2012;30(15):1770—1776.
4. Fokas E, Liersch T, Fietkau R, et al. Tumor regression grading after preoperative chemoradiotherapy for locally advanced rectal carcinoma revisited: updated results of the CAO/ARO/AIO-94 trial. *J Clin Oncol*. 2014;32(15):1554—1562.
5. Patel UB, Taylor F, Blomqvist L, et al. Magnetic resonance imaging-detected tumor response for locally advanced rectal cancer predicts survival outcomes: MERCURY experience. *J Clin Oncol*. 2011;29(28):3753—3760.
6. Capirci C, Valentini V, Cionini L, et al. Prognostic value of pathologic complete response after neoadjuvant therapy in locally advanced rectal cancer: long-term analysis of 566 ypCR patients. *Int J Radiat Oncol Biol Phys*. 2008;72(1):99—107.
7. O'Connell MJ, Colangelo LH, Beart RW, et al. Capecitabine and oxaliplatin in the preoperative multimodality treatment of rectal cancer: surgical end points from national surgical adjuvant breast and bowel project trial R-04. *J Clin Oncol*. 2014;32(18):1927—1934.
8. Chow OS, Kuk D, Keskin M, et al. KRAS and combined KRAS/TP53 mutations in locally advanced rectal cancer are independently associated with decreased response to neoadjuvant therapy. *Ann Surg Oncol*. 2016;23(8):2548—2555.
9. Sclafani F, Gonzalez D, Cunningham D, et al. TP53 mutational status and cetuximab benefit in rectal cancer: 5-year results of the EXPERT-C trial. *J Natl Cancer Inst*. 2014;106(7):dju121.
10. Duldulao MP, Lee W, Nelson RA, et al. Mutations in specific codons of the KRAS oncogene are associated with variable resistance to neoadjuvant chemoradiation therapy in patients with rectal adenocarcinoma. *Ann Surg Oncol*. 2013;20(7):2166—2171.
11. Kamran SC, Lennerz JK, Margolis CA, et al. Integrative molecular characterization of resistance to neoadjuvant chemoradiation in rectal cancer. *Clin Cancer Res*. 2019;25(18):5561—5571.
12. Bengala C, Bettelli S, Bertolini F, et al. Prognostic role of EGFR gene copy number and KRAS mutation in patients with locally advanced rectal cancer treated with preoperative chemoradiotherapy. *Br J Cancer*. 2010;103(7):1019—1024.
13. Dejea CM, Wick EC, Hechenbleikner EM, et al. Microbiota organization is a distinct feature of proximal colorectal cancers. *Proc Natl Acad Sci U S A*. 2014;111(51):18321—18326.
14. Keku TO, Dulal S, Deveaux A, et al. The gastrointestinal microbiota and colorectal cancer. *Am J Physiol Liver Physiol*. 2015;308(5):G351—G363.
15. Russo E, Taddei A, Ringressi MN, et al. The interplay between the microbiome and the adaptive immune response in cancer development. *Therap Adv Gastroenterol*. 2016;9(4):594—605.
16. Iida N, Dzutsev A, Stewart CA, et al. Commensal bacteria control cancer response to therapy by modulating the tumor microenvironment. *Science*. 2013;342(6161):967—970.
17. Sivan A, Corrales L, Hubert N, et al. Commensal Bifidobacterium promotes antitumor immunity and facilitates anti-PD-L1 efficacy. *Science*. 2015;350(6264):1084—1089.
18. Kostic AD, Gevers D, Pedamallu CS, et al. Genomic analysis identifies association of Fusobacterium with colorectal carcinoma. *Genome Res*. 2012;22(2):292—298.
19. Castellarin M, Warren RL, Freeman JD, et al. Fusobacterium nucleatum infection is prevalent in human colorectal carcinoma. *Genome Res*. 2012;22(2):299—306.
20. Mima K, Nishihara R, Qian ZR, et al. *Fusobacterium nucleatum* in colorectal carcinoma tissue and patient prognosis. *Gut*. 2016;65(12):1973—1980.
21. Bullman S, Pedamallu CS, Sicinska E, et al. Analysis of *Fusobacterium* persistence and antibiotic response in colorectal cancer. *Science*. 2017;358(6369):1443—1448.
22. Yu T, Guo F, Yu Y, et al. Fusobacterium nucleatum promotes chemoresistance to colorectal cancer by modulating autophagy. *Cell*. 2017;170(3):548—563.e16.
23. Shang FM, Liu HL. Fusobacterium nucleatum and colorectal cancer: a review. *World J Gastrointest Oncol*. 2018;10(3):71—81.
24. Mima K, Sukawa Y, Nishihara R, et al. Fusobacterium nucleatum and T cells in colorectal carcinoma. *JAMA Oncol*. 2015;1(5):653—661.

25. Mima K, Cao Y, Chan AT, et al. Fusobacterium nucleatum in colorectal carcinoma tissue according to tumor location. *Clin Transl Gastroenterol*. 2016;7(11):e200.
26. Ito M, Kanno S, Nosho K, et al. Association of *Fusobacterium nucleatum* with clinical and molecular features in colorectal serrated pathway. *Int J Cancer*. 2015;137(6):1258—1268.
27. Tahara T, Yamamoto E, Suzuki H, et al. Fusobacterium in colonic flora and molecular features of colorectal carcinoma. *Cancer Res*. 2014;74(5):1311—1318.
28. Gaulke CA, Sharpton TJ. The influence of ethnicity and geography on human gut microbiome composition. *Nat Med*. 2018;24(10):1495—1496.
29. Deschasaux M, Bouter KE, Prodan A, et al. Depicting the composition of gut microbiota in a population with varied ethnic origins but shared geography. *Nat Med*. 2018;24(10):1526—1531.
30. Dayde D, Tanaka I, Jain R, et al. Predictive and prognostic molecular biomarkers for response to neoadjuvant chemoradiation in rectal cancer. *Int J Mol Sci*. 2017;18(3):573.
31. Helleday T. Making immunotherapy "cold" tumors "hot" by chemotherapy-induced mutations-a misconception. *Ann Oncol*. 2019;30(3):360—361.
32. Matsutani S, Shibutani M, Maeda K, et al. Significance of tumor-infiltrating lymphocytes before and after neoadjuvant therapy for rectal cancer. *Cancer Sci*. 2018;109(4):966—979.
33. Kaplan CW, Ma X, Paranjpe A, et al. Fusobacterium nucleatum outer membrane proteins Fap2 and RadD induce cell death in human lymphocytes. *Infect Immun*. 2010;78(11):4773—4778.
34. Chen T, Li Q, Wu J, et al. Fusobacterium nucleatum promotes M2 polarization of macrophages in the microenvironment of colorectal tumors via a TLR4-dependent mechanism. *Cancer Immunol Immunother*. 2018;67(10):1635—1646.
35. Gur C, Ibrahim Y, Isaacson B, et al. Binding of the Fap2 protein of Fusobacterium nucleatum to human inhibitory receptor tigit protects tumors from immune cell attack. *Immunity*. 2015;42(2):344—355.